Nuclear and charge density distributions in ferroelectric $PbTiO_3$: maximum entropy method analysis of neutron and X-ray diffraction data

Jinlong Zhu,[1,2] Wei Han,[2] Jianzhong Zhang,[1] Hongwu Xu,[1] Sven C. Vogel,[1] Changqing Jin,[2,a)] Fujio Izumi,[3] Koichi Momma,[3,b)] Yukihiko Kawamura,[3,c)] and Yusheng Zhao[1,2,4,a)]
[1]*LANSCE and EES Division, Los Alamos National Laboratory, Los Alamos, New Mexico 87545*
[2]*National Laboratory for Condensed Matter Physics, Institute of Physics, CAS, Beijing 100190, China*
[3]*National Institute for Materials Science, 1-1Namiki, Tsukuba, Ibaraki 305-0044, Japan*
[4]*HiPSEC, Department of Physics and Astronomy, University of Nevada, Las Vegas, Nevada 89154*

(Received 10 April 2013; accepted 27 July 2013)

We conducted *in-situ* high-temperature neutron and X-ray diffraction studies on tetragonal $PbTiO_3$. Using a combination of Rietveld analysis and Maximum Entropy Method, the nuclear and charge density distributions were determined as a function of temperature up to 460 °C. The ionic states obtained from charge density distributions reveal that the covalency of Pb–O_2 bonds gradually weakens with increasing temperature. The spontaneous polarizations calculated from the contributions of ionic state, ionic displacement, and nuclear polarization, are in good agreement with the experimental measurements. This method provides an effective approach to determine spontaneous polarizations in multiferroics with high-current leakage and low resistance. © *2013 International Centre for Diffraction Data*. [doi:10.1017/S0885715613000675]

Key words: ferroelectric materials, neutron diffraction, X-ray diffraction

I. INTRODUCTION

The maximum entropy method (MEM) is an effective way to establish models from a finite number of observed physical quantities by maximizing information entropy (Izumi, 2004) By combining MEM (Sakata and Sato, 1990) with the Rietveld refinement (Rietveld, 1969), one can determine three-dimensional (3D) charge and nuclear density distributions from X-ray and neutron diffraction data, respectively. This technique has extensively been applied to structural studies of manganites (Takata *et al.*, 1999), ferroelectric perovskites, (Kuroiwa *et al.*, 2001; Aoyagi *et al.*, 2002) ionic conductors, (Nishimura *et al.*, 2008; Yashima, 2009) and clathrates (Hoshikawa *et al.*, 2005; Igawa *et al.*, 2010). For instance, MEM can reveal electronic orbital hybridization and orbital ordering from a limited amount of X-ray diffraction data (Takata *et al.*, 1999; Kuroiwa *et al.*, 2001; Aoyagi *et al.*, 2002). MEM can also resolve possible ionic pathways in ionic or mixed conductors and gas molecular distributions in clathrates (Hoshikawa *et al.*, 2005; Nishimura *et al.*, 2008; Yashima, 2009; Igawa *et al.*, 2010). Therefore, the MEM/Rietveld analysis is a very powerful approach to reconstruct the atom distribution and interatomic charge densities associated with thermal motion and phase transition.

In the present study, we choose $PbTiO_3$, a classic and extensively studied ferroelectric material (Shirane and Hoshino, 1951; Glazer and Mabud, 1978; Fontana *et al.*, 1990; Cohen, 1992), to corroborate the origin of tetragonal ferroelectric distortion, electron and nuclear distributions, and spontaneous polarization. All of these properties can be derived and calculated by the MEM/Rietveld analysis of neutron and X-ray diffractions. It is well known that at room temperature $PbTiO_3$ possesses a tetragonal structure with an axial ratio of $c/a = 1.06$ (Shirane and Hoshino, 1951), distorted from the cubic, paraelectric phase below the Curie temperature of 490 °C. In ABO_3 ferroelectric perovskite such as $BaTiO_3$ and $KNbO_3$, the anisotropic distortion of tetragonal phase from cubic phase arises from the covalent nature of B–O bonds. It has been pointed out that the hybridization between the Ti 3*d* states and O 2*p* states is essential to the ferroelectric instability in $PbTiO_3$ (Cohen, 1992). In $PbTiO_3$, the $6s^2$ lone-pair effect from Pb^{2+} gives rise to additional distortion (Kuroiwa *et al.*, 2001), which results in high spontaneous polarization in the tetragonal phase. There are two distinct atomic positions for oxygen in the crystal structure of tetragonal $PbTiO_3$. The Pb–O_2 bonds (parallel to the *c*-axis) are covalent, whereas the Pb–O_1 bonds (normal to the *c*-axis) are ionic. Direct visualization of temperature-dependent nuclear and electron distributions will not only help understand the observed structural and electronic behaviors, but will also be essential for validating first-principles calculations from local bonding characteristics to 3D unit-cell models.

We performed *in situ* neutron and X-ray diffraction experiments to investigate the evolution of nuclear and charge densities of $PbTiO_3$ as a function of temperature. The MEM/Rietveld analysis of neutron diffraction data provides an insight into the nuclear configuration, relative atom position

a)Authors to whom correspondence should be addressed. Electronic mail: jin@iphy.ac.cn; Yusheng.Zhao@unlv.edu
b)Present address: National Museum of Nature and Science, 4-1-1 Amakubo, Tsukuba, Ibaraki 305-0005, Japan.
c)Present address: Research Center for Neutron Science and Technology, Comprehensive Research Organization for Science and Society, 162-1 Shirane Shirakata, Tokai-mura, Naka-gun, Ibaraki 319-1106, Japan.

distributions, and anisotropic thermal motion. From the X-ray diffraction data one can determine the charge density distributions around the atomic nuclei, bonding characteristics from interatomic charge densities, strength of covalent nature, as well as the effective ionic charges. Most importantly, spontaneous polarization can be deduced from the nuclear and charge distributions.

II. EXPERIMENTAL

Phase-pure tetragonal $PbTiO_3$ powders were obtained from Alfa Aesar (99.9% metal based purity). The high-temperature neutron diffraction experiment was conducted with an ILL-type furnace (Vogel *et al.*, 2004) at the flightpath of High-Pressure-Preferred Orientation (HIPPO) (Wenk *et al.*, 2003; Vogel *et al.*, 2004), Los Alamos Neutron Science Center (LANSCE). The sample was loaded into a vanadium can of 1 cm diameter, which has low attenuation for neutrons and can hold temperature up to 1200 °C. The time-of-flight neutron diffraction data were collected with three detector banks at Bragg angles of $2\theta = 144.45°$, 90.00°, and 39.30°, covering the *d*-spacing range of 0.58–4.8 Å. The high-temperature X-ray diffraction experiment was performed in a Philips X'pert diffractometer using Cu$K\alpha_1$ radiation. Diffraction data were collected at steps of 0.03°, and the counting time was 5 s for each step. The Rietveld analyses were performed using the General Structure Analysis System (GSAS) program software package (Larson and Von Dreele, 2004). Observed structure factors, F_o, and standard uncertainties, $\sigma(|F_o|)$, which were estimated with Alchemy (Izumi and Kawamura, 2006) from relevant data in files output by GSAS, were analyzed by the MEM with Dysnomia (Izumi and Momma, 2011). In MEM analysis, we used all three banks of neutron data with carefully selected TOF regions and X-ray diffraction data in a scanning range of $2\theta = 10$–135°, corresponding to the *d*-spacing range of 0.77–4.44 Å. The unit cell was divided into $128 \times 128 \times 134$ for the tetragonal $PbTiO_3$. The detailed method for MEM analysis can be found in Ref. (Izumi and Momma, 2011).

III. RESULTS AND DISCUSSION

The Rietveld refinements of neutron and X-ray diffraction data for tetragonal $PbTiO_3$ at room temperature are shown in Figures 1(a) and 1(b), respectively. The intensity residual values, R_B, for all of the refinements are smaller than 5%, which indicates reasonable agreement between the experimental data and structural model for the title compound. The refinements with fairly low R_B values also provide good starting points for the subsequent MEM analysis. For neutron diffraction, the use of data from multi-detector banks, as shown in the inset of Figure 1(a), can minimize the complication from background and region of overlapping reflection to obtain more accurate nuclear density distributions.

Figure 2 shows nuclear density distributions at four different temperatures of tetragonal $PbTiO_3$ in one unit cell with an isosurface level of 0.1 fm/Å^3; the 3D visualization was conducted by VESTA (Momma and Izumi, 2011). The (blue) balls in the unit-cell center are Ti ions with a negative neutron scattering length. The Pb ions are located at the unit-cell corners. The O ions are on the six surface planes. For clearer discussion, the two O ions on the (0 0 1) planes are denoted as

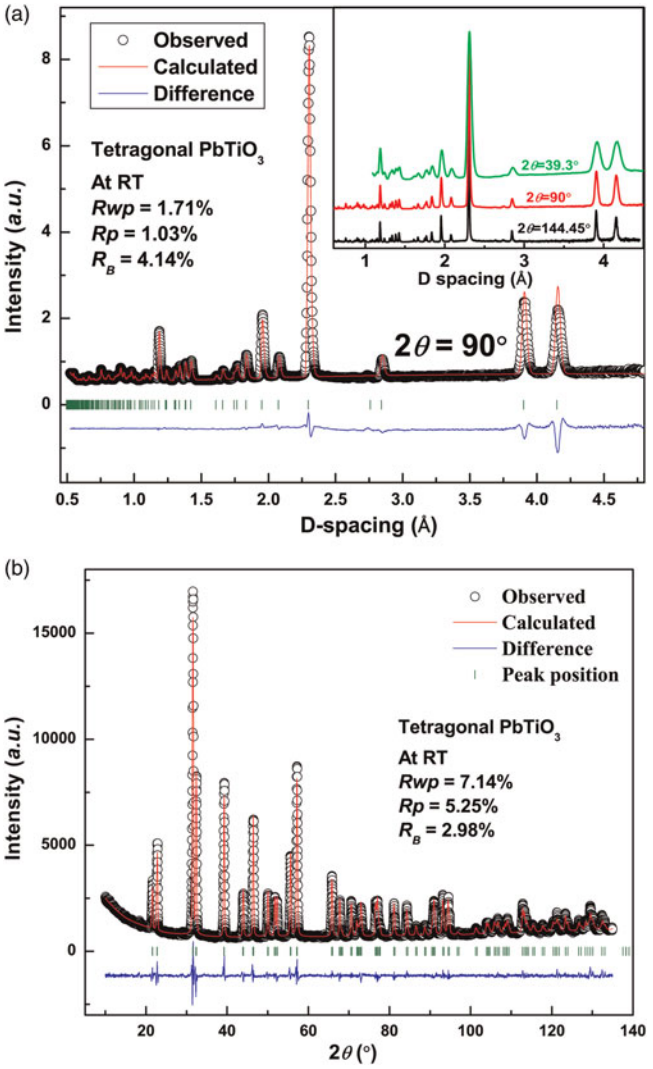

Figure 1. Rietveld refinements of neutron (a) and X-ray diffraction data (b); for tetragonal $PbTiO_3$. Inset of (a) shows diffraction patterns from three different detector banks, which are combined for the MEM analysis.

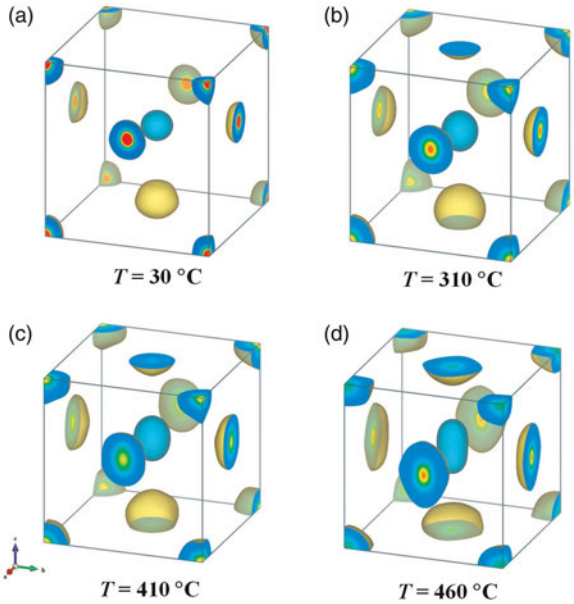

Figure 2. 3D nuclear density distributions of tetragonal $PbTiO_3$ at 30, 310, 410, and 460 °C, all at an isosurface level of 0.1 fm/Å^3.

https://doi.org/10.1017/S0885715613000675 Published online by Cambridge University Press

O_1, and the rest of O ions on the (1 0 0) and (0 1 0) planes are denoted as O_2. An inspection of Figure 2 indicates that the nuclear density distributions for all atoms expand with increasing temperature as a result of thermal vibrations. The expansion, however, is substantially more pronounced for Ti and O atoms than for Pb atoms. Note that O and Ti atoms also have a similar anisotropic temperature factor. The nuclear density distribution for O_2 atoms stretches symmetrically along the *c*-axis and has an egg-shaped geometry. On the other hand, the O_1 atoms gradually elongate along the *b*-axis with increasing temperature and eventually are pan-caked at 460 °C. This behavior indicates that the interaction between Ti and O_2 is different from that between Ti and O_1, which is further confirmed by the charge density analysis, as will be discussed below. The relatively smaller nuclear density distribution for Pb atoms indicates that the interaction between Ti and O is stronger than that between Pb and O. For all three atoms, the shape evolutions are consistent with the mean-square thermal amplitude variations reported for single-crystal $PbTiO_3$ (Nelmes and Kuhs, 1985).

MEM analysis of X-ray diffraction data is a straightforward approach to derive the interatomic charge-density distributions and hence the interaction and bonding characteristics between adjacent atoms. Figure 3 shows the charge-density distributions for $PbTiO_3$ at four different temperatures, all with an isosurface level of 0.8 e/Å^3. Figures 4(a)–4(c) display the 2D charge density configurations in the range of 0–1.0 e/Å^3 for (0 0 1), (1 0 0), and (0 2 0) lattice planes, respectively. It is evident from Figure 4(a) that there is no charge density overlap between neighboring Pb and O_1, indicating an ionic nature for the Pb–O_1 bonds. The Pb–O_2 bond is covalent with ~0.17 e/Å^3 charge density value in critical point, as revealed by the charge density distributions on the (1 0 0) lattice plane in Figure 4(b). The Ti–O bond is also covalent with ~0.75 e/Å^3 charge density value in critical point, relatively stronger than the Pb–O_2 bond as shown in Figure 4(c). In titanate perovskite such as $PbTiO_3$ and $BaTiO_3$, the Ti–O covalent bonding is primarily responsible for ferroelectric polarization, whereas the Pb–O_2 covalent bonding presents a large energy barrier for the ferroelectric to paraelectric phase transition (Kuroiwa *et al.*, 2001). Figure 4(d) shows the charge density distributions and atom positions of $PbTiO_3$ at room temperature. The 3D vision of the charge density geometry of $PbTiO_3$ unit cell is straightforward and clear to describe the bond characters.

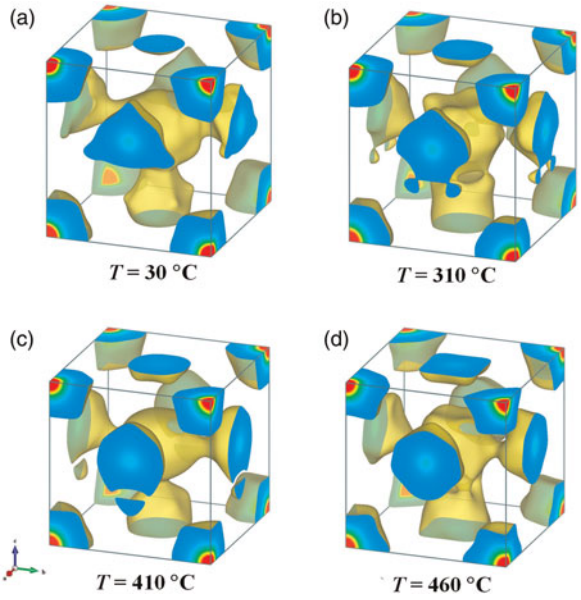

Figure 3. 3D charge density distributions of tetragonal $PbTiO_3$ at 30, 310, 410, and 460 °C, all with an isosurface level of 0.8 *e*/Å^3.

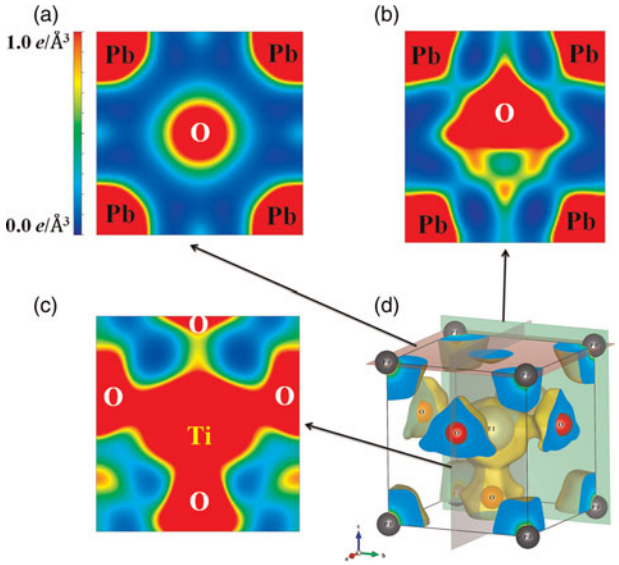

Figure 4. 2D charge density configurations of $PbTiO_3$ at 30 °C in the range of 0–1.0 e/Å^3. The images of (a), (b), and (c) correspond to the (0 0 1), (1 0 0), and (0 2 0) lattice planes, respectively, as illustrated in (d). Figure 4(d) also shows charge density distributions and positions of the constituent atoms in 3D version.

The bond lengths determined from our neutron diffraction data for Pb–O_1, Pb–O_2, Ti–O_1, and Ti–O_2 are 2.79(1) , 2.52 (1), 1.76(3), and 1.97(2) Å, at room temperature and are 2.80(2), 2.82(1), 1.94(1), and 1.98(2) Å, respectively, at 460°. The relatively large increase in Ti–O_1 and Pb–O_2 bond lengths indicates that both tetragonal distortion and bonding strength decrease with increasing temperature. To further describe the bonding character at elevated temperature, the ionic states of constituent atoms were calculated by counting the numbers of charges around the atoms with a minimum charge density surface as a boundary condition. The spontaneous polarization of tetragonal $PbTiO_3$ was then calculated from two distinct components: the ionic polarization calculated from the effective ionic states of constituent atoms and displacements of Pb and Ti sublattices relative to the oxygen octahedron (Kuroiwa *et al.*, 2001); the electron polarization of all atoms, which was calculated from the relative shift of the electrons (X-ray refinements) to the nuclear position (neutron diffraction refinements). Briefly, the ionic spontaneous polarization is calculated by multiplying the effective charges and the distance between the negative and positive valence weighted mean center along the *c*-axis then dividing by the volume of the unit cell. The electron polarisation is the sum of the contribution of each constituent ion: the total electrons of each ion times the distance between the electrons center (negative charge) and nuclear center (positive charge) along *c*-axis and then divided by the volume of the unit cell. The effective ionic valence and spontaneous polarization

https://doi.org/10.1017/S0885715613000675 Published online by Cambridge University Press

TABLE I. Effective charges and ionic states (in parentheses) of constituent atoms and polarizations in tetragonal $PbTiO_3$ as a function of temperature. The polarization is calculated from the ionic states, ionic displacements, and relative shifts between electron and nucleus positions. The ionic polarization values in the brackets are only from charge densities derived from X-ray diffractions.

$PbTiO_3$	Pb	Ti	O_1	O_2	Polarization(ionic polarization) ($\mu C/cm^2$)
30 °C	81.0 (+1.0)	19.6 (+2.4)	9.4 (−1.4)	9.0 (−1.0)	64.8 (32.4)
310 °C	80.4 (+1.6)	29.6 (+2.4)	9.4 (−1.4)	9.3 (−1.3)	47.2 (31.6)
410 °C	80.2 (+1.8)	19.5 (+2.4)	9.5 (−1.4)	9.4 (−1.4)	30.5 (28.7)
460 °C	80.2 (+1.8)	19.5 (+2.5)	9.5 (−1.5)	9.4 (−1.4)	17.8 (21.8)

calculated for tetragonal $PbTiO_3$ at different temperatures are listed in Table I. With increasing temperature from 30 to 460 °C, the ionic state changes from +1 to +1.8 for Pb and from −1 to −1.4 for O_2. The ionic states of Ti and O_1 are essentially unchanged in this temperature range. The results indicate that the covalency of the Pb–O_2 bond is suppressed with increasing temperature. Eventually, after phase transition above 490 °C, the Pb–O_2 bond becomes ionic in the cubic phase (Kuroiwa *et al.*, 2001). The calculated spontaneous polarization from the charge distributions only at room temperature is 32.4 $\mu C/cm^2$, which is consistent with the conclusion in (Kuroiwa *et al.*, 2001), but it is far less than total polarization obtained from the experimental measurements (Gavrilyachenko *et al.*, 1970; Remeika and Glass, 1970). This indicates that the relative shifts of electrons from nuclei cannot be ignored. By taking the advantage of MEM analysis of neutron and X-ray diffraction data, we can calculate the contribution of such shifts to spontaneous polarization. The thus-calculated total spontaneous polarization for tetragonal $PbTiO_3$ is 64.8 $\mu C/cm^2$ at room temperature, which agrees with those obtained from dielectric hysteresis loop measurements, 75 $\mu C/cm^2$ (Gavrilyachenko *et al.*, 1970) and 57 $\mu C/cm^2$ (Remeika and Glass, 1970). The calculated spontaneous polarization decreases rapidly with increasing temperature, indicating that the electrons are more symmetrically distributed around the nuclei at elevated temperature. This behavior dominates the contribution to spontaneous polarization even though the effective ionicity increases with increasing temperature.

IV. CONCLUSION

In summary, by a combination of MEM and Rietveld analyses of neutron and X-ray diffraction data, spontaneous polarization for ferroelectric $PbTiO_3$ was accurately determined. This method would be particularly useful and effective for the study of multiferroics as an experimental measurement of polarization is greatly hindered and screened by the low electrical resistance and high-current leakage in bulk samples. In addition, MEM analysis of neutron and X-ray diffraction data can offer accurate structural and electronic parameters for verifying theoretical models and predictions.

ACKNOWLEDGEMENTS

This work was supported by the laboratory-directed research and development (LDRD) program of Los Alamos National Laboratory, which is operated by Los Alamos National Security LLC under DOE contract no. DE-AC52-06NA25396. The experimental work has benefited from the use of the Lujan Neutron Scattering Center at Los Alamos Neutron Science Center, which is funded by the US Department of Energy's Office of Basic Energy Sciences. The work at IOPCAS was supported by NSF & MOST through the research projects.

Aoyagi, S., Kuroiwa, Y., Sawada, A., Tanaka, H., Harada, J., Nishibori, E., Takata, M., and Sakata, M. (**2002**). "Direct observation of covalency between O and disordered Pb in Cubic $PbZrO_3$," J. Phys. Soc. Jpn. **71**, 2353–2356.

Cohen, R. E. (**1992**). "Origin of ferroelectricity in perovskite oxides," Nature (London) **358**, 136–138.

Fontana, M. D., Idrissi, H., and Wojcik, K. (**1990**). "Displacive to order-disorder crossover in the Cubic-Tetragonal phase transition of $PbTiO_3$," Europhys. Lett. **11**, 419–424.

Gavrilyachenko, V. G., Spinko, R. I., Martynenko, M. A., and Fesenko, E. G. (**1970**). "Spontaneous polarization and coercive field of lead titanate," Sov. Phys. Solid State **12**, 1203.

Glazer, A. M. and Mabud, S. A. (**1978**). "Powder profile refinement of lead zirconate titanate at several temperatures. II. Pure $PbTiO_3$," Acta Crystallogr. B **34**, 1065–1070.

Hoshikawa, A., Igawa, N., Yamauchi, H., and Ishii, Y. (**2005**). "Neutron powder diffraction study of methane deuterohydrate by the maximum entropy method," J. Phys. Chem. Sol. **66**, 1810–1814.

Igawa, N., Taguchi, T., Hoshikawa, A., Fukazawa, H., Yamauchi, H., Utsumi, W., and Ishii, Y. (**2010**). "CO_2 motion in carbon dioxide deuterohydrate determined by applying maximum entropy method to neutron powder diffraction data," J. Phys. Chem. Sol. **71**, 899–905.

Izumi, F. (**2004**). "Beyond the ability of Rietveld analysis: MEM-based pattern fitting," Solid State Ionics **172**, 1–6.

Izumi, F. and Kawamura, Y. (**2006**). "Three-dimensional visualization of nuclear densities by MEM analysis from time-of-flight neutron powder diffraction data," Bunseki Kagaku **55**, 391–395.

Izumi, F. and Momma, K. (**2011**). "Three-dimensional visualization of electron- and nuclear-density distributions in inorganic materials by MEM-based technology," IOP Conf. Ser.: Mater. Sci. Eng. **18**, 022001.

Kuroiwa, Y., Aoyagi, S., Sawada, A., Harada, J., Nishibori, E., Takata, M., and Sakata, M. (**2001**). "Evidence for Pb-O covalency in tetragonal $PbTiO_3$," Phys. Rev. Lett. **87**, 217601.

Larson, A. C. and Von Dreele, R. B. (**2004**). *General Structure Analysis System (GSAS)* (Report LAUR 86-748). Los Alamos, New Mexico: Los Alamos National Laboratory.

Momma, K. and Izumi, F. (**2011**). "VESTA 3 for three-dimensional visualization of crystal volumetric and morphology data," J. Appl. Crystallogr. **44**, 1272–1276.

Nelmes, R. J. and Kuhs, W. F. (**1985**). "The crystal structure of tetragonal $PbTiO_3$ at room temperature and at 700 K," Sol. Stat. Commun. **54**, 721–723.

Nishimura, S., Kobayashi, G., Ohoyama, K., Kanno, R., Yashima, M., and Yamada, A. (**2008**). "Experimental visualization of lithium diffusion in Li_xFePO_4," Nat. Mater. **7**, 707–711.

Remeika, J. P. and Glass, A. M. (**1970**). "The growth and ferroelectric properties of high resistivity single crystals of lead titanate," Mater. Res. Bull. **5**, 37–45.

Rietveld, H. M. (**1969**). "A profile refinement method for nuclear and magnetic structures," J. Appl. Crystallogr. **2**, 65–71.

Sakata, M. and Sato, M. (**1990**). "Accurate structure analysis by the maximum-entropy method," Acta Crystallogr. Sect. A **46**, 263–270.

Shirane, G. and Hoshino, S. (**1951**). "On the phase transition in lead titanate," J. Phys. Soc. Jpn. **6**, 265–270.

Takata, M., Nishibori, E., Kato, K., Sakata, M., and Moritomo, Y. (**1999**). "Direct observation of orbital order in manganites by MEM charge-density study," J. Phys. Soc. Jpn. **68**, 2190–2193.

Vogel, S. C., Hartig, C., Lutterotti, L., Von Dreele, R. B., Wenk, H. R., and Williams, D. J. (**2004**). "Texture measurements using the new neutron diffractometer HIPPO and their analysis using the Rietveld method," Powder Diffr. **19**, 65–68.

Wenk, H.-R., Lutterotti, L., and Vogel, S. (**2003**). "Texture analysis with the new HIPPO TOF diffractometer," Nucl. Instrum. Methods Phys. Res., Sect. A **515**, 575–588.

Yashima, M. (**2009**). "Diffusion pathway of mobile ions and crystal structure of ionic and mixed conductors – A brief review," J. Ceram. Soc. Jpn. **117**, 1055–1059.

https://doi.org/10.1017/S0885715613000675 Published online by Cambridge University Press